Materials Research Proceedings 28 (2023) 249-258 https://doi.org/10.21741/9781644902479-27

Feasibility study of compression molding for large reinforcement structures in the commercial vehicle sector

LÜCKENKÖTTER Julian[1,a *], LEIMBACH Jan-Patrick[2,b], STALLMEISTER Tim[1,c], MARTEN Thorsten[1,d] and TRÖSTER Thomas[1,e]

[1]Paderborn University, Chair of Automotive Lightweight Design, Warburger Str. 100, 33098 Paderborn, Germany

[2]LIA GmbH, Hohenloher Weg 16, 33102 Paderborn, Germany

[a]julian.lueckenkoetter@upb.de, [b]jan.leimbach@lia-group.de, [c]tim.stallmeister@upb.de, [d]thorsten.marten@upb.de, [e]thomas.troester@upb.de

Keywords: Compression Molding, Fiber Content, Process Development, Lightweight Design

Abstract. Due to an increasing volume of shipments, there is a significant need for more delivery vehicles. One approach to reduce the associated increase in carbon dioxide (CO_2) emissions is a new light weight design approach involving the substitution of conventional materials with glass fiber mat-reinforced thermoplastics (GMT) based on polypropylene (PP). The application of GMT by compression molding is a widely used process in the automotive industry. However, application in the commercial vehicle sector requires much larger dimensions, making it necessary to clarify whether the manufacturing process and material are suitable for semi-structural applications on this scale. To find this out, two replacement geometries are abstracted in this study and manufactured by varying the main manufacturing parameters. The feasibility can be demonstrated by recording and analyzing the resulting process variables and measuring the formed fiber distribution. At the end of the paper, recommendations are given for the production of GMT structures on the scale of commercial vehicles.

Introduction

Background.

Current studies on the development of parcel services clearly show that national and international shipment volumes have risen sharply in recent years and continue to rise further. While 2.4 billion shipments were delivered in Germany in 2011, the total increased to 4.5 billion in 2021. Compared with the previous year 2020, this represents an increase of 11.2 %. By 2026, the volume of shipments is forecast to reach around 5.7 billion [1]. To cope with the growing volume of shipments, significantly more delivery vehicles will be needed. In addition to high investments, the increasing volume of traffic also leads to greater strain on the infrastructure in inner-city traffic. This in turn results in longer idle times for all road users and increased emissions of greenhouse gases, which are crucial to climate change. For this reason, it is a necessary consequence to reduce the emission of climate-damaging combustion gases such as CO_2.

Two thirds of the vehicle fleet of parcel services consists of light commercial vehicles. These include commercial vehicles with a gross vehicle weight of up to 7.5 tons [2]. Current floor assemblies for box bodies of these light commercial vehicles consist of numerous individual parts, which entails many manufacturing and assembly steps. This is not only time-consuming but also cost-intensive. Furthermore, the lightweight potential of such bodies is limited and therefore requires a new and systemic development approach.

Project approach.

In this project, a process is to be developed that allows the modular subdivision of the loading floor for light commercial vehicles. For this purpose, an integral design with materials not commonly used for this area will be applied. By reducing the vehicle weight, the mass-dependent driving resistances correlating with CO_2 emissions can be minimized and the assembly effort for the floor structure can be kept to a minimum [3]. On the other hand, the lower unladen weight of the vehicle means that more parcels can be moved with a single vehicle, so that in total fewer delivery vehicles need to be used to cope with the increasing volume of parcels (cf. Fig. 1a).

Within the scope of the project, the floor modules will be manufactured from GMT, which is processed by compression molding (cf. Fig. 1b). The PP based material offers excellent weight specific mechanical properties, outstanding cost efficiency and a high degree of design freedom. The advantages over thermosets are based on shorter process times, almost unlimited recyclability and higher toughness [4-6]. Compression molding is well established and has been used in the automotive industry for many years. The heated GMT cuttings are pressed into cavities at forming pressures of up to 200 bar, so that complex structural components can be produced via flow movements of the material [4, 5]. Furthermore, due to the higher fiber length compared to fiber-reinforced granules in injection molding, higher mechanical strengths can be generated [6].

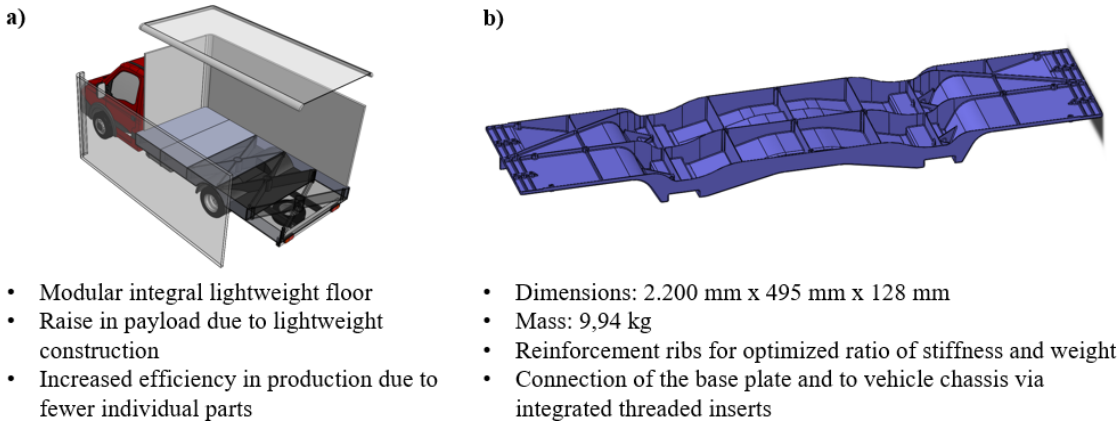

Fig. 1. a) Illustration of a commercial vehicle up to 3.5 t with box body and the associated project goals b) Design model of the floor module based on GMT.

Fig. 1b) shows the current design status of the topology-optimized CAD model of the floor module. The opposing requirements for stiffness and minimum weight can be met via reinforcement ribs. By stringing together eight modules, the entire store floor of the delivery vehicle is represented. A base plate can be mounted using threaded inserts integrated in the compression molding process. On the underside, the modules can be connected to the different geometries of the vehicle manufacturers underbodies.

Experimental Approach

To validate the process concept, it is necessary to investigate whether compression molding of GMT is suitable for the large dimensions of commercial vehicle sector in terms of mold filling and homogeneous fiber distribution. As shown in [4], the filling of the cavity in the course of the material flow movement can lead to accumulation of glass fibers in some places and thus to voids in other places of the component. These phenomena correlate with the final mechanical properties of the component. Rubio et. al. [5] found that the simpler the geometry, the more homogeneous the resulting properties are. Pöhler [7] investigated the fiber content of compression molded reinforcement ribs with a length of 90 mm as a function of the geometric design parameters. With a nominal fiber content of about 52 %, the fiber content in the rib tip was reduced up to 30 %. For

a compromise between lightweight construction and homogeneous cavity filling, Pöhler defined a demolding angle of 1.0 °, a minimum rib width of 3.0 mm and an insertion radius of 6.0 mm [7].

Rib geometry.

Since no comparable work is available for rib lengths greater than 90 mm, two different rib lengths are considered in this study and need to be investigated. As the final geometry of the floor module had not yet been determined at the time the tests were carried out, the rib lengths 87 mm and 200 mm were selected in order to be able to analyze a clear influence of the rib lengths. The rib length L, which is more than twice as long, is compensated by an increased demolding angle α and width W at the uppermost point. The minimum rib thickness is identical. Since a modular compression molding tool is used, other main dimensions of the rib are identical (cf. Fig. 2 a-b) and Fig. 3 a-c). A list of all different parameters is given in Table 1.

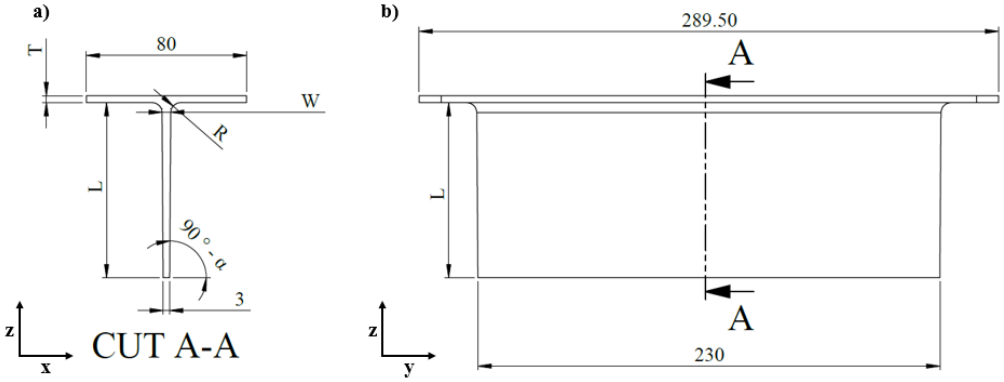

Fig. 2. Dimension of investigated ribs with a) cut view and b) longitudinal view.

Table 1. Parameters of "Rib 87 mm" and "Rib 200 mm".

Parameter	**Rib 87 mm**	**Rib 200 mm**
Rib length L	87 mm	200.0 mm
Insertion radius R	5.0 mm	6.0 mm
Rib width top W	4.3 mm	9.8 mm
Demolding angle α	0.4 °	1.0 °
Flange thickness T	Depending on material insert and mold filling (1.7 mm – 11.5 mm)	

Process technology.

The used compression molding tool can hold various cavities due to the pocket in the lower mold plate. Temperature regulation up to 95°C is enabled via a water-based temperature control unit. A cutout of the same size as the face of the cavity is provided in the upper mold plate, so that sealing of the process via vertical flash faces is possible (cf. Fig. 3 a).

Holes for piezoelectric pressure sensors are recessed at various positions within the cavities so that the resulting pressure in the cavity can be measured. In the cavity for the shorter rib length, holes are also provided for temperature sensors at the same position on the opposite cavity wall. In both cavities, two temperature sensors are positioned at the lowest point parallel to the direction of material flow in order to be able to measure the temperature of the melt shortly before the mold is completely filled (cf. Fig. 3 b-c).

As in Stallmeister et. al. [8], piezoelectric load cells are used to record the resulting press force and a draw-wire sensor is used to detect the press stroke. The data from the pressure sensors, the load cells and the draw-wire sensor are recorded simultaneously, so that no time offset has to be considered in the analysis.

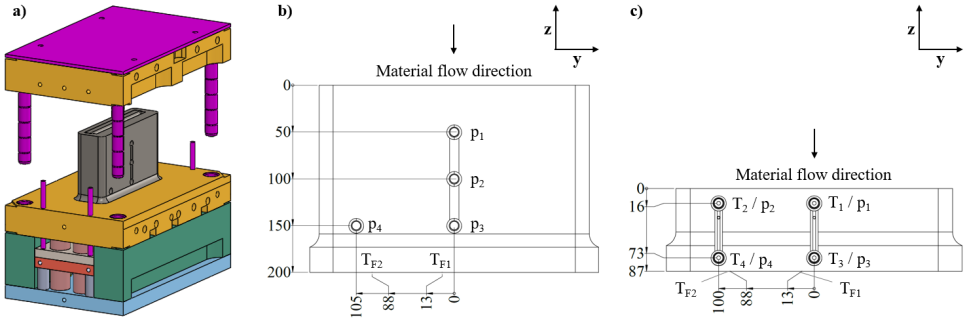

Fig. 3. a) Compression molding tool and b) – c) cavities with the respective geometric positions of the sensors.

Materials.

A widely used PP-based GMT with a fiber mass fraction of 52 % from Mitsubishi Chemicals Advanced Materials (MCAM) is used for the majority of the tests. According to the manufacturer, the material has good flow properties, a very homogeneous fiber distribution and is applied for semi-structural applications. A GMT with 33% fiber mass fraction from MCAM is used to analyze the flow behavior as a function of the fiber content. The main properties can be found in Table 2.

Table 2. Material properties of the GMT used according to MCAM.

Material properties	**GMT PP-GF52**	**GMT PP-GF33**
Thickness (laminate)	4.8 mm	5.4 mm
Density (laminate)	1.34 g/cm³	1.12 g/cm³
Density (molded)	1.40 g/cm³	1.16 g/cm³
Tensile strength	145 MPa	70 MPa
Tensile modulus	8600 MPa	4600 MPa
Melting point	165°C	166°C

Process sequence.

GMT cuttings with the dimensions of 260 mm x 50 mm are used for specimen production. To achieve a defined mass for the specific trial, smaller sheets are added until the desired weight is reached. Fig. 4 a-d) shows the following process steps.

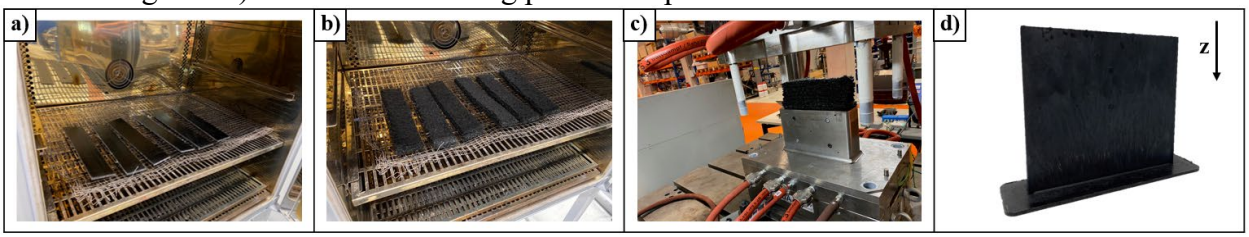

Fig. 4. Process sequence: a) GMT in furnace, b) heated GMT, c) GMT stack on cavity, d) manufactured rib.

The cuttings are placed next to each other in a 250°C convection oven and are heated for 10 minutes (cf. Fig. 4 a-b) Before transfer to the compression molding tool, the sheets are stacked in the oven to minimize temperature loss to the ambient air. After the GMT stack is centered on the cavity, the press stroke of a hydraulic forming press with a maximum press force of 50 tons is immediately actuated to form the rib (cf. Fig. 4 c-d). Closing speed of the press is about 30 mm / sec. The press force F is calibrated based on the desired forming pressure p, which is calculated from the press force F and the projected area of the cavity A_{cav}, before the test (cf. Eq. 1).

Forming pressure p is maintained for a time s of approx. 60 seconds. After completion of the pressing process, the rib is ejected via the ejector unit of the tool.

$$p = \frac{F}{A_{cav}} \tag{1}$$

Process Parameters.

In order to obtain various information on mold filling and fiber distribution in the ribs, applied forming pressures (100, 150 and 200 bar), mass of the inserted material (approx. 450-650 g) and temperature of the cavity (25°C and 90°C) for GMT PP-GF52 are systematically varied. The cavity temperatures 25°C and 90°C are marked T_{25} and T_{90} in the following. The investigations are mainly concentrated on the 200 mm long rib type and are occasionally carried out for the 87 mm long rib type (approx. 350 g – 400 g of GMT). Furthermore, the influence of a reduced fiber mass fraction (33 %) is investigated for defined test points. Each test point is performed at least twice.

Analysis methods.

To evaluate the quality of the ribs, the complete shape was visually inspected. In this context, it is useful to determine the resulting flange thickness by measuring the local thickness in at least three places and then calculating an average value. Furthermore, the resulting pressures in the cavity are analyzed as a function of the geometric position in the cavity. By means of the temperature measurements within the tool, it is possible to estimate the flowability of the GMT melt.

In order to gain an insight into the resulting fiber contents and distributions, X-rays of the ribs and point density measurements as a function of cavity depth are performed. While 2D X-ray is very well suited for the detection of fiber accumulations and voids, density measurement allows a quantitative and time-saving measurement of the resulting fiber content, since a determination of fiber content via ashing method according to DIN ISO 1172 [9] is too time-consuming for the large number of samples (up to 120 specimens). PP has a density of approx. 0.9 g/cm³ and E-glass fibers of approximately 2.6 g/cm³ [4]. Considering the specification for the pressed laminate, fiber accumulation or voids can be classified numerically (cf. Table 2). This is done by measuring the mass of the sample in ambient air (m_{GMT}) and under complete coverage with a known fluid (m_F). The difference between the masses is the mass of the displaced fluid. By dividing with the known density of the fluid ρ_F (in this case ethanol), the volume of the displaced fluid and thus the volume of the specimen V_{GMT} can be determined. Afterwards, the density ρ_{GMT} of the body can be calculated (cf. Eq. 2) [10].

$$\rho_{GMT} = \frac{m_{GMT}}{V_{GMT}} = \frac{m_{GMT}}{\frac{m_{GMT} - m_F}{\rho_F}} = \frac{m_{GMT} * \rho_F}{m_{GMT} - m_F} \tag{2}$$

Results

Mold filling.

In the following, only the results for complete shaped ribs with a length of 200 mm and the material PP-GF52 are considered, since mold filling for the 87 mm long rib is already state of the art. The heated GMT stack has an approximate temperature of 200°C before insertion, which was determined in advance with an infrared camera. At a forming pressure of 100 bar and a low cavity temperature (T_{25}), the mold filling can be improved with increased GMT mass (450-660 g), but a complete mold formation is not possible (cf. Fig. 5 a-c). Instead, the resulting flange thickness grows with increasing material input (up to 8.2 mm). If the temperature of the cavity is increased (T_{90}), complete mold formation is already possible from an inserted mass of 450 g. For this material input, the resulting flange thickness is reduced from approx. 3.2 mm (T_{25}) to 2.0 mm (T_{90}).

At a forming pressure of 150 bar, mold formation is possible from a GMT mass of 490 g (T_{25}). A positive influence on mold formation can be observed due to the lower flange thickness (2.1 mm

at 450 g GMT mass). Once again, complete mold formation is possible with a mass of 450 g when the cavity is heated up (T_{90}).

If the forming pressure is increased to 200 bar, complete ribs are possible in some cases from a mass of 450 g (T_{25}). Reliable mold filling can also be achieved starting from a mass of approx. 490 g (cf. Fig. 5 d). Variations between individual test points may be due to different transfer times and resulting temperature losses.

Basically, it can be stated that mold tempering is very advantageous for complete mold formation. It is also advisable to increase the forming pressure and the insertion mass. However, it must be considered that the increased GMT mass can lead to an undesirably high wall thickness in real components.

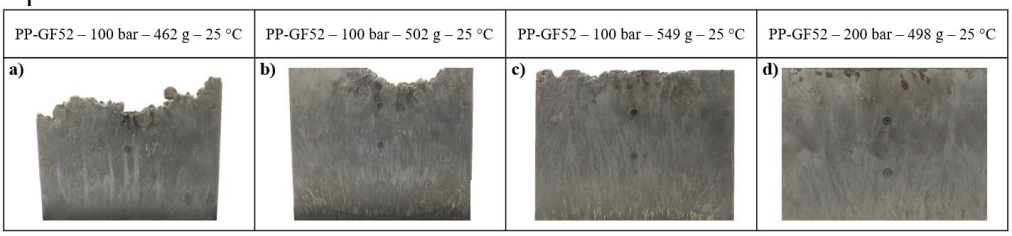

Fig. 5. Mold filling of the 200 mm long rib for selected process parameter combinations a) – d).

Process Monitoring.

Fig. 6 shows the recorded process parameters for the rib geometry with a length of 200 mm produced from GMT PP-GF52. The calculated forming pressure p, the measured values of cavity pressure p_1 – p_4 and the temperature T_{F1} – T_{F2} in the base of the rib as a function of time t are presented for two different combinations of process parameters (cf. Fig. 6 a-b). Since the calculated forming pressure p is proportional to the press force F, the force is not shown separately (cf. Eq. 1). Furthermore, the recorded press stroke changes only minimally as soon as the maximum press pressure has been applied, so this is also not shown. The process start is defined as soon as the measured force rises.

Forming pressure.

In both diagrams it is visible that forming pressure drops minimally after a steep start. Subsequently, the desired forming pressure level is reached with a reduced gradient. This phenomenon is due to the fact that the stacked GMT layers are initially compressed and start to enter the cavity since the mentioned threshold value is reached. After a compression time of at least 60 seconds, the process is terminated.

Cavity pressure.

With a small time offset, which is based on the distance between the insertion radius and the 1st pressure sensor, the cavity pressure at sensor p_1 increases with a similar slope. It is noticeable that the maximum pressure in the cavity is clearly below the calculated forming pressure. Furthermore, it is visible that the pressure p_1 does not remain constant and decreases over time. The qualitative trend of the sensors p_2 - p_4 corresponds essentially to the described trend of p_1. However, there is a premature pressure drop with increasing cavity depth (p_2, p_3/p_4) and nearness to the outer wall (p_4). This effect will be due to the thermal shrinkage of the GMT, as the material thickness decreases with increasing cavity depth, allowing the heat to dissipate faster. Furthermore, the heat can be dissipated even better at the outer edges of the cavity, so that full pressure drop occurs first at sensor p_4 (cf. Fig. 6 a-b).

Furthermore, a fundamental difference can be observed in the characteristics of the cavity pressures for different process parameters. While the cavity pressures p_1-p_4 at a forming pressure of 150 bar for a high cavity temperature (T_{90}) start almost simultaneously and reach a common maximum (cf. Fig. 6 a), a clear time offset in the pressure rise and a difference in the respective maxima can be seen at a pressure of 100 bar and a low cavity temperature (T_{25}). In addition, the

cavity pressures are maintained for a significantly shorter time and are significantly lower in relation to the calculated pressure (cf. Fig. 6 b).

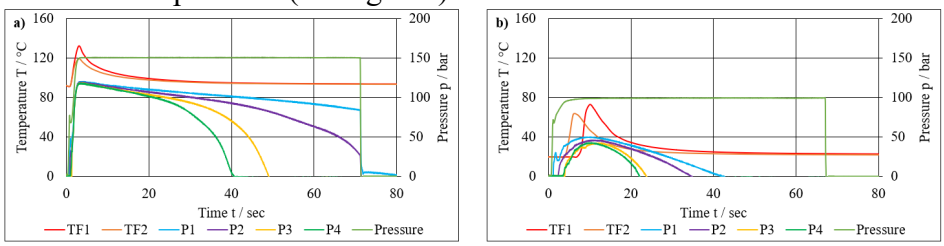

Fig. 6. Process diagrams with parameter combinations a) 150 bar, 649 g, T_{90} and b) 100 bar, 662 g, T_{25}.

Temperatures.

Examination of the resulting temperature in the base of the rib at two positions provides information about the temperature of the melt - and thus the flowability of the GMT - and about the geometric characteristics of the flow front. In the case of Fig. 6 a) both sensors reach their maximum almost simultaneously. However, the temperature at the sensor with the smaller wall distance is about 10 K lower. Compared to the set cavity temperature, there is an offset of 30-40 K. In comparison with other forming pressures and GMT masses, no significant differences can be observed.

In the second example (cf. Fig. 6 b), the maxima of the temperature sensors occur with a time offset. Here, the melt seems to first hit the sensor in the outer areas of the cavity wall. Compared to T_{25}-cavity wall, the maximum temperature offset is 40-50 K. At a maximum of 70°C, the temperature of the material is significantly below the melting temperature of the material, so that a clearly poorer flowability can be concluded.

For temperature sensors T1-T4, which are aligned orthogonally to the press direction of the 87 mm long rib, temperature offset of the GMT is even lower to the prevailing temperature in the tool (cf. Fig. 3 c). If the cavity is not heated, the maximum measured temperature is 40°C. If the cavity is heated to 90°C, the temperature of GMT is 100°C. It can be concluded from this that the outermost layer of material solidifies immediately on the cavity wall and the molding is driven from inside the structure.

Further analysis of cavity pressure.

As can be seen in Fig. 6, the measured cavity pressure sometimes differs significantly from the calculated forming pressure p. Insufficient pressure within the cavity can result in the GMT not being properly compacted. As a consequence, air pockets and fiber accumulations could result, since the pressure is not high enough to push fibers all the way to the bottom. In order to investigate this in more detail, the maximum ratio of the acting pressure ratio $p_{r,max}$ was determined for all test points for the pressure sensor p_1 (cf. Eq. 1 and 3).

$$p_{r,max} = \frac{p_{1,max}}{p_{max}} \tag{3}$$

Fig. 7 below shows this ratio as a function of inserted GMT mass, rib length, glass fiber content and cavity temperature for both rib types. Low values for a 200 mm long rib for a cavity temperature of 25°C (cf. Fig. 7 a) are due to insufficient mold filling. It can be observed that the ratio can be increased up to 0.75 when the forming pressure and GMT mass are increased. A further increase is possible with a tempered cavity, but the maximum is at a value of about 0.85 (cf. Fig. 8 b). The above-mentioned ratios can be achieved with a reduced fiber content (PP 33) even with significantly lower GMT masses (cf. Fig. 7 a-b).

Much less mass is required for the mold filling of the 87 mm long rib. Specimens prepared show that ratios of up to 92 % can be achieved even at low forming pressures and when using

GMT PP-GF52 (PP 52). At cavity temperature of 90°C and use of GMT PP-GF33 (PP 33), even a ratio of 1.0 is possible (cf. Fig 7 a-b).

From the results, it is concluded that the moldability of GMT is more advantageous with lower fiber content and shorter ribs. This is justified by the lower flow resistance due to reduced fiber content and shorter material flow paths. The impact of a reduced pressure ratio on the mechanical properties must be determined by separate investigations.

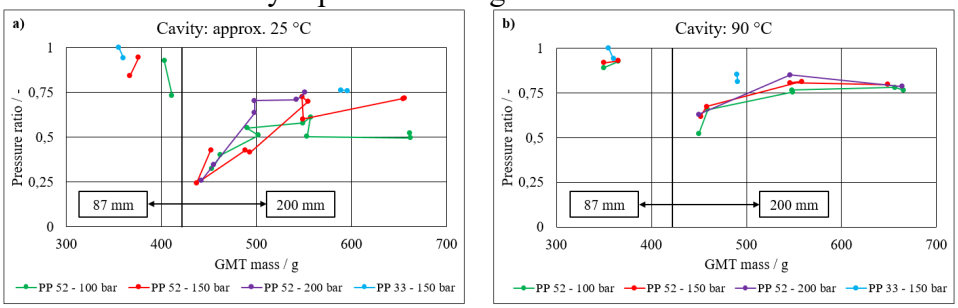

Fig. 7. Maximum pressure ratio of sensor p_1 as a function of process parameters for a) cavity temperature of approx. 25°C and b) cavity temperature of 90°C.

Qualitative fiber distribution.

A low pressure ratio could mean that a homogeneous fiber distribution might not be present for a rib length of 200 mm. To investigate this in more detail, the results of the X-ray images of the ribs are presented and analyzed below.

When analyzing the X-ray images of the 200 mm long ribs (cf. Fig. 8 a-e), it is noticeable that for the most part there is a very homogeneous fiber distribution. Only at a forming pressure of 150 bar and a low material loading of 488 g there are larger voids (cf. Fig 8 a). Smaller voids in the base of the ribs cannot be completely eliminated for PP-GF52 by increasing forming pressure, GMT mass and cavity temperature (cf. Fig. 8 b-c). In comparison, there appear to be fewer voids for a PP-GF33 (cf. Fig. 8 d). Increasing the temperature to 90 °C almost completely eliminates them (cf. Fig. 8 e).

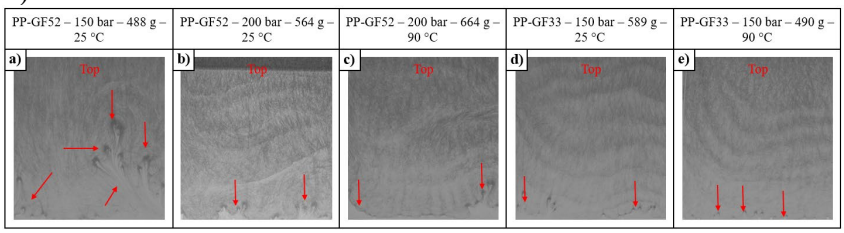

Fig. 8. X-rays of the ribs with a length of 200 mm for different parameter combinations a)-e). The full height (200 mm) and approx. half of the width (145 mm) are shown starting from the cavity wall.

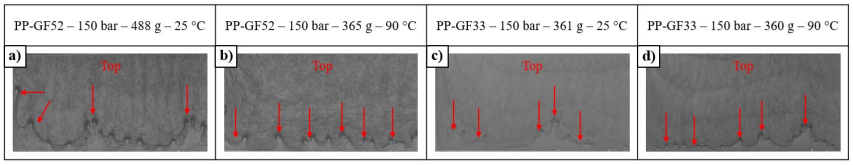

Fig. 9. X-rays of the ribs with a length of 87 mm for different parameter combinations a)-d). The full height (87 mm) and approx. 75% of the width (217 mm) are shown starting from the cavity wall.

In relation to the total rib length, the voids are significantly more pronounced in the 87 mm ribs (cf. Fig. 9 a-d). For PP-GF52, minimization is possible by increasing the cavity temperature

(cf. Fig. 9 a-b). For PP-GF33, the voids are again smaller, but complete elimination is not possible by tempering the cavity (cf. Fig. 9 c-d).

Quantitative fiber distribution.

To determine the density, the ribs are divided into rectangular test pieces. For ribs with a length of 200 mm, the test pieces have a size of 20 mm x 20 mm and for ribs with a length of 87 mm a size of 10 mm (parallel to flow direction) x 20 mm. For comparison, an average value is calculated for each height row (cf. Fig 10 a-b).

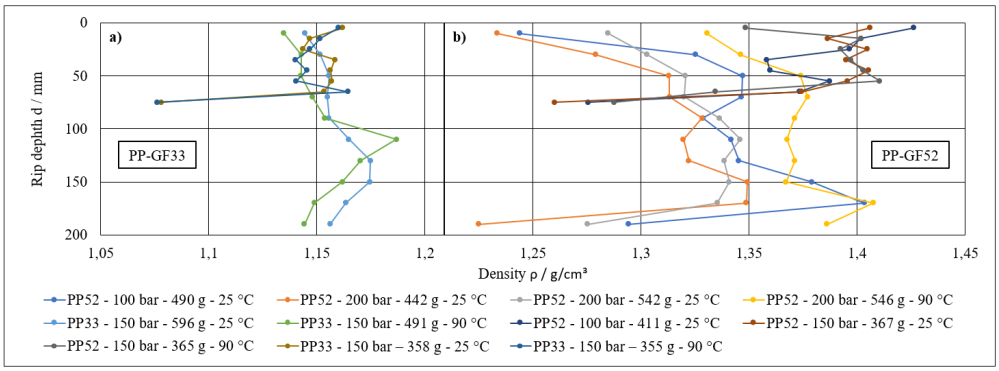

Fig. 10. Density measurements for both rib types with materials a) PP-GF33 and b) PP-GF52.

For rib length 200 mm, it is noticeable that the density, despite decreasing cavity pressure, rises continuously with increasing rib depth. When using PP-GF52, the density is many times below the value from the data sheet for the starting material. It is possible that the prevailing pressure is not sufficient to cause enough compression for the large wall thicknesses. A lack of glass fibers is unlikely at this point (cf. Fig. 10 b). For PP-GF33, the density is more homogeneous, with a tendency to increase as well (cf. Fig. 10 a).

In the deepest row, the density for PP-GF52 is significantly lower than in the penultimate row for many ribs. This will be due to the voids detected in the X-ray image. In contrast, for a high forming pressure and a tempered cavity, almost no drop is observed and the density value corresponds to the data plot for molded GMT. Obviously, an increased forming pressure, a sufficient amount of GMT and a tempered cavity leads to a satisfying compression and fiber distribution in the material (cf. Fig. 10 b).

For the 87 mm long rib, the value for compressed GMT from the data sheet is achieved (almost) for all specimens in the first row. With decreasing rib depth, this remains relatively constant and decreases again more strongly in the last row. In this application, a strong decrease is also observed for PP-GF32 (cf. Fig. 10 a-b). Basically, the findings made correlate well with the X-ray images and the certain pressure ratios. Voids occur only in the lowest areas and are more pronounced in the geometry of an 87 mm long rib. This can be answered by the low demolding angle. Furthermore, the increased pressure ratios for the GF-PP33 and the 87 mm long rib result in improved compression. This can be compensated for a 200 mm long rib by a high forming pressure and tempering of the cavity. A sufficient amount of GMT is also essential.

Summary

In the research project, floor modules for delivery vehicles should be produced from GMT using the compression molding process. Due to the dimensions prevailing in the commercial vehicle sector and a topology optimization carried out, reinforcing ribs up to a length of 200 mm may be required to meet the mechanical requirements. This goes beyond the previous state of the art, so that it was necessary in this study to abstract two substitute geometries of the floor module and to

test the process for its suitability for this application scenario by varying the most significant process parameters (e.g. forming pressure, mass, temperature of cavity, fiber content).

By analyzing the mold filling, the resulting process parameters (e.g. resulting pressures and temperatures in the cavity) and methods for qualitative and quantitative determination of the fiber distribution, a basic feasibility for the application in the commercial vehicle sector can be demonstrated. To prevent voids without any fibers, it must be ensured that the demolding angle of the cavity is greater than or equal to 1 °, sufficient amount of GMT is used (≥ 450 g), high forming pressure (≥ 150 bar) is applied and that the tool is heated (≥ 90 °C).

The knowledge gained will be used for further design of the floor module. Nevertheless, further mechanical tests will have to be carried out to confirm the study carried out. Moreover, a process simulation with the 3DTimon software will be validated on the basis of the recorded measurement data. This is to be used in the final stage to predict the manufacturing process of the whole floor module.

Acknowledgement
The research project is funded by the German Federal Ministry for Economic Affairs and Climate Action as part of "Technologietransfer-Programm Leichtbau". Thanks are due to all project members not mentioned by name. Special thanks go to Dr. Manel Ellouz of Bielefeld University of Applied Sciences for her support in the preparation and discussion of the X-ray images.

References
[1] KE-CONSULT Kurte&Esser GbR, KEP-Studie 2022 - Analyse des Marktes in Deutschland, Cologne, 2022.
[2] KE-CONSULT Kurte & Esser GbR, BIEK Kompendium Teil 2, 2018.
[3] B. Klein, T. Gänsicke, Leichtbau-Konstruktion. Dimensionierung, Strukturen, Werkstoffe und Gestaltung, eleventh ed., Springer Vieweg, Wiesbaden, 2018. https://doi.org/10.1007/978-3-658-26846-6
[4] AVK – Industrievereinigung Verstärkte Kunststoffe e. V., Handbuch Faserverbundkunststoffe / Composites, fourth ed., Springer Vieweg, Wiesbaden, 2014. https://doi.org/10.1007/978-3-658-02755-1
[5] A. Rubio, P. Eguizabal, M.A. Mendizabal and J.F. Liceaga, Influence of the processing parameters on glass mat reinforced thermoplastic (GMT) stamping, Compos. Manuf. 3 (1992) 47-52. https://doi.org/10.1016/0956-7143(92)90183-U
[6] J.L. Thomason, The influence of fibre length and concentration on the properties of glass fibre reinforced polypropylene: 5. Injection moulded long and short fibre PP, Compos. Part A 33 (2002) 1641-1652. https://doi.org/10.1016/S1359-835X(02)00179-3
[7] S. Pöhler, Konzeptionierung und Auslegung eines Vorderachsträgers in hybrider Leichtbauweise im C-Segment, Shaker-Verlag, Düren, 2021. ISBN: 9783844082104
[8] T. Stallmeister, T. Tröster, In-Mold-Assembly of Hybrid Bending Structures by Compression Molding. Key Eng. Mater. 926 (2022) 1457-1467. https://doi.org/10.4028/p-5fxp53
[9] DIN EN ISO 1172:1998-12, Prepregs, Formmassen und Laminate; Bestimmung des Textilglas- und Mineralfüllstoffgehalts, Beuth Verlag GmbH, Berlin, 1998.
[10] Information on http://www.tomchemie.de/Mathe/3.1.3/3.1.3.htm (accessed 31 January 2023).